TECTONICS, VOL. 8, NO. 2, PAGES 333-350, APRIL 1989

THE ANATOMY OF A PULL-APART BASIN: SEISMIC REFLECTION OBSERVATIONS OF THE DEAD SEA BASIN

Uri S. ten Brink[1] and Zvi Ben-Avraham

Department of Geophysics and Planetary Sciences, Tel Aviv University, Ramat Aviv, Israel

Abstract. The Dead Sea Basin (DSB), located along the African-Arabian plate boundary, constitutes a good example of a pull-apart basin because of its large dimensions, its structural simplicity, and its active subsidence. A coherent three-dimensional picture of the DSB has been constructed on the basis of analysis of seismic stratigraphy together with the interpretation of previously published geological and geophysical data. Despite the large known vertical offsets across the basin, deformation takes place mainly along the transverse and longitudinal faults, and the intervening sediments are relatively undeformed and are hardly tilted. Comparison between E-W seismic lines indicate that the basin has widened by the collapse and tilting of arcuate blocks from the western margin but that its original shape is a full-graben. The southern and central parts of the basin are divided into equidistant segments 20-30 km long by transverse faults. Activity along these faults commenced only during the Pleistocene, long after the Dead Sea strike-slip fault system was formed, and migrated northward with time. A likely scenario for the development of the DSB is one in which the basin grows northward with time by a simultaneous propagation of the southern strand of the Dead Sea fault and a retardation of the northern strand.

[1]Now at Department of Geophysics, Stanford University, Stanford, California.

Paper number 88TC04028.
0278-7407/89/88TC-04028$10.00

INTRODUCTION

Strike-slip faults of great linear extent are often associated with a wide range of structural styles of deformation including normal and reverse faults, en echelon folds, tension cracks, splay faults, and rotated blocks [Wilcox et al., 1973; Freund, 1974; Harding et al., 1985]. Among the distinct structures associated with strike-slip faults are sedimentary basins which vary in length from tens of meters to few hundred kilometers [Mann et al., 1983] and have a proportionally smaller width (a ratio of 1:3 according to Aydin and Nur [1982]). The larger-scale basins (> 10 km) reach a depth of several kilometers (e.g., Ventura Basin [Yeats, 1983] Western Imperial valley [Johnson et al., 1983] Los Angeles basin [Crowell, 1974] Soledad basin [Muehlberger, 1958] and Hula, Sea of Galilee, and the Dead Sea [Kashai and Crocker, 1987]) while basins on the scale of 5-10 km reach a depth of a few hundred meters (e.g., Cholame valley [K. Shedlock et al., manuscript in preparation, 1988], Bir Zreir [Eyal et al., 1986]).

One of the largest (110 x 16 km) and deepest (8-10 km) active strike-slip basins currently known is the Dead Sea Basin (DSB)[Aydin and Nur, 1982]. The basin is located along the Dead Sea strike-slip fault system, a plate boundary which separates Arabia from Africa and Sinai and connects the incipient mid-oceanic ridge of the Red Sea to the collision and subduction belt of southern Turkey (Figure 1). The basin makes a topographic depression 400 m below sea level and is composed of two subbasins; the southern subbasin is subaerial, and the northern subbasin is occupied by a lake, which bottoms at a depth of 725 m below sea level (Figure 1).

Indirect evidence [Sa'ar, 1985] places the age of at least part of the Hazeva formation, the lowermost unit found within the DSB, in the middle Miocene and even earlier. The Hazeva formation, which unconformably overlies Senonian and Eocene rocks, represents a period of continental, fluviatile, and lacustrine sedimentation [Kashai, 1989]. Its thickness varies

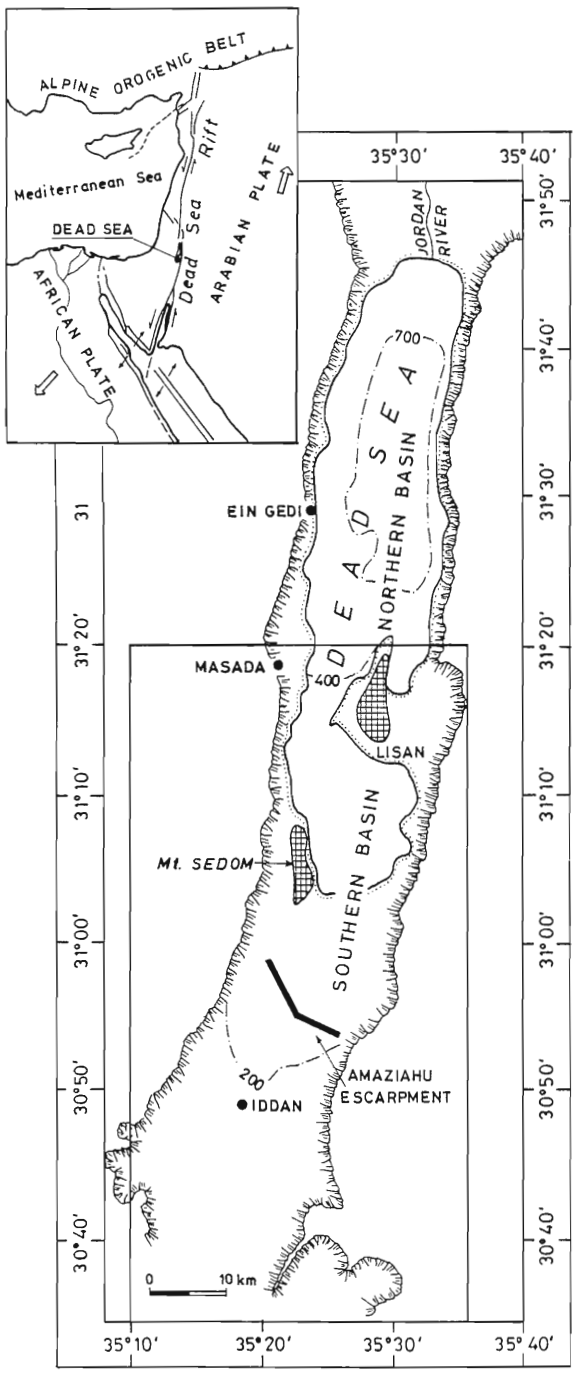

Fig. 1. (opposite) Map of the Dead Sea basin. The northern part of the basin, below an elevation of -400 m, is occupied by a lake, known as the Dead Sea (shorelines are dotted). The hatched lines mark the topographic escarpment, a few hundred meters high in places, which delimits the basin. Elevations are below sea level. The grated areas denote salt diapirs. The area within the box is shown in Figure 2. The location of the Dead Sea basin within the Dead Sea strike-slip system (also known as the Dead Sea Rift) is shown in the inset (modified from Garfunkel et al., [1981]).

between 150 m and 660 m in the southern part of the DSB but the formation is absent further north within the basin (in Ein Gedi borehole near Ein Gedi, Figure 1). The Hazeva formation is also found in the surrounding areas of the Negev, eastern Sinai, and Jordan, thus indicating that deposition during the Miocene was not confined to the DSB . We therefore regard the Hazeva Formation as part of the basement and not as part of the DSB sedimentary fill. It is noteworthy that there is contradictory evidence from an ancient drainage system of the existence of a basin along the whole length of the DSB during the Early Miocene [Garfunkel and Horowitz, 1966].

Unlike the Hazeva formation, the geographical distribution of the Sedom formation of middle to late Pliocene shows that its deposition is clearly related to the subsidence of the DSB [Zak, 1967]. The Sedom formation is mostly composed of evaporites (mainly salt) which form two large diapirs in the central part of the DSB (Mount Sedom and the Lisan, Figure 1). The nearly 1000 m of salt encountered in the Amiaz borehole (Figure 2) may be either part of the nearby Mount Sedom diapir or represent the average thickness of Sedom Formation in the basin. The Amora Formation of Pleistocene age is a thick (at least 3500 m in the Melech Sedom borehole in the center of the basin, Figure 2 [Kashai and Crocker, 1987] section of lacustrine and evaporitic carbonates and fluvial clastics [Zak and Freund, 1981]. The Amora formation is covered by 100-150 m of the Lisan Formation, the deposits of a Wurm Stage lake.

The active subsidence of the DSB is evident from the surface topography, exposed faults, seismic activity [e.g., Rotstein and Arieh, 1986] and the thick Pleistocene clastic sequence recovered in drill holes. Unlike some of the southern California basins which have been overthrusted subsequent to their formation (e.g. Ventura basin [Yeats, 1983]) the DSB, as will be shown, is characterized by little internal deformation. The DSB with its current subsidence, large dimensions, and relative structural simplicity is therefore a suitable case study of the structure and evolution of pull-apart basins. The purpose of this paper is to reconstruct the internal anatomy of the DSB in light of newly available multichannel seismic reflection data. In particular, we shall examine the mode and timing of deformation as they are revealed by seismic stratigraphy in the basin and compare the observations to existing models of the development of strike-slip basins.

THE INDUSTRY SEISMIC REFLECTION DATA

Numerous multichannel seismic profiles were collected and processed by oil companies over the last decade in the DSB. We chose to analyze a selected subset of these profiles that provide an aerial grid within the southern and central parts of the basin (Figure 2). This subset of profiles is usually of the highest quality available in the area in terms of both the acquisition parameters and the processing. The energy sources for the profiles were either Vibroseis systems with 39-7 Hz sweep, 15-20 sweeps per vibrator point, or dynamite shots detonated simultaneously in 3-5 holes, 1.2-kg charge per hole. The profiles were recorded by 48 and 96 channel arrays, often in split profile configurations,with a typical recording time of 4-6 s. Shot point and receiver station spacings varied between 36 m and 50 m. Standard exploration processing was applied to these profiles. In our analysis we used unmigrated and time

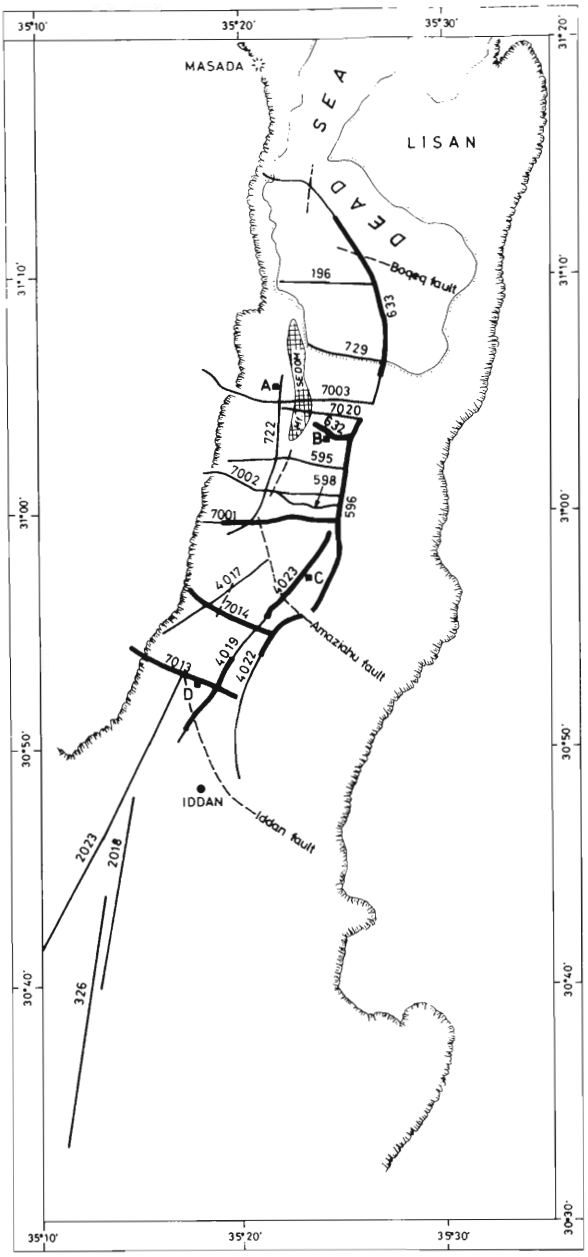

Fig. 2. Location map of the multichannel seismic reflection lines analyzed in the present work. Thicker lines denote line segments shown in Figures 3 to 8. Correlation of seismic reflection lines and subsurface geology utilized deep commercial boreholes marked by solid squares: A, Amiaz borehole; B, Melech Sedom borehole; C, Amaziahu borehole; D, Arava borehole. The thin dashed lines mark the surface traces of faults which were intersected by the seismic lines. Hatched and dotted lines are as in Figure 1.

migrated versions of these profiles. Some of the profiles, often with differing interpretations, have been published previously [Ginzburg and Kashai, 1981; Arbenz, 1984; Kashai and Crocker, 1987; Kashai, 1989].

OBSERVATIONS

Transverse Faults

Three transverse (diagonal) fault zones cut the southern part of the DSB in a SSE-NNW direction (Figure 2), and separate it into three segments. The faults from south to north are (1) subsurface fault, named here the Iddan fault, delimiting the DSB in the south, (2) the Amaziahu fault [Neev and Emery, 1967] which is accompanied by a 50 m high escarpment, and (3) the Boqeq fault [Z. Ben-Avraham et al., Transverse faults at the northern end of the southern basin of the Dead Sea graben, submitted to *Tectonophysics*, 1988] south of the Lisan peninsula. The Amaziahu fault will be described first because of the superior quality of seismic lines crossing it and will be followed by the Iddan and the Boqeq faults, respectively.

The Amaziahu fault appears in the seismic reflection profiles (Figure 3 and 4) as a spectacular low-angle normal fault, which may be traced from the surface down to a depth of 3.4 s two-way travel time. The sedimentary infill above this fault is deformed by fractures and detached antithetic normal faults. The basement underlying the fault zone (B in Figure 3 and 4) appears to be cut by normal (?) faults which offset both horizontal and tilted blocks. The basement is identified here and throughout the paper by its prominent wavy appearance and is often overlain by base-lapping reflectors. The surface trace of the Amaziahu fault is curvilinear in the direction NW to NNW (Figure 2) and the escarpment retains a constant elevation along this trace. Comparison between the seismic profiles (Figure 3 and 4), all of which cross the fault at close to a perpendicular angle, shows progressive steepening of the fault dip toward the west (i.e., a spoon-shaped fault). The smallest dip is found in the profile oriented in a NNE-SSW direction, crossing the fault at the center of the basin (Figure 3), and the steepest dip is found in the line 7001 (Figure 4) oriented E-W and crossing the fault where it intersects or merges with the western longitudinal fault.

The dip of the Amaziahu listric fault, which is steep near the surface, bends rather abruptly at 1.8 s (Figure 4). We interpret this change in dip to be caused by the intersection of the fault plane with the salt layer of Sedom formation (the sequence between B and S4 in line 4023, Figure 4, see correlation below). Northward and eastward the Amaziahu fault plane merges into the salt layer, which appears to follow the topography of the basement faults (Figures 3 and 4).

The Iddan fault separates about 2 s of coherent reflections, which are interpreted as basin fill, from the area to the southeast which lacks coherent reflections (Figure 5). Over 2.7 km of basin fill were indeed found in Arava 1 borehole (marked D in Figure 2), which is within the area of coherent reflections (Figure 5). In contrast, the Miocene age Hazeva formation is exposed in the area lacking coherent reflections [Bentor et al., 1965], and this area is thus considered to lie outside the basin. The fault in line 4019 (Figure 5) terminates about 0.6 s below the surface, and shallower reflections appear to be flexed but not offset. The southern shores of the Holocene Lake Lisan have extended over the fault [Begin et al., 1974] and a surficial fault trace cannot be identified. Basin fill is observed all the way to the southernmost end of line 4022 (see Figure 2 for location) indicating that the basin is longer at its center than at its western side. A curvilinear surficial trace

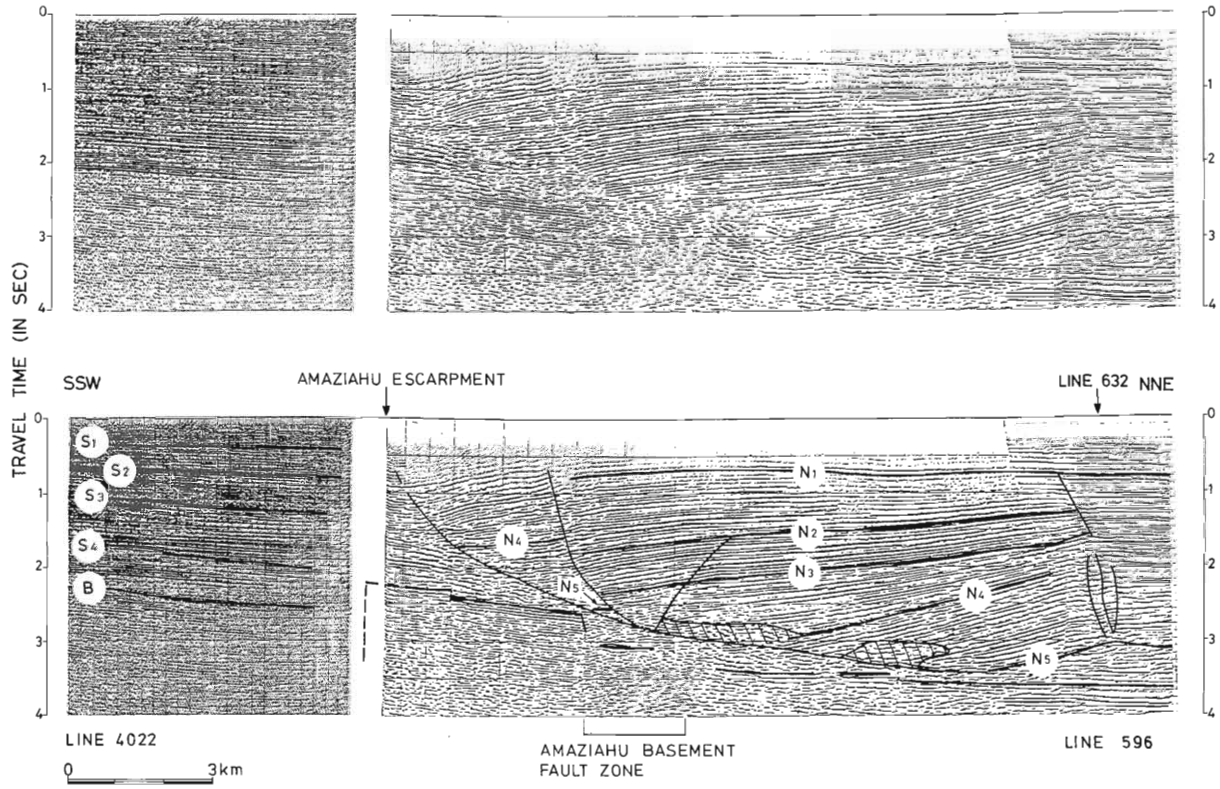

Fig. 3. Portions of migrated seismic lines 4022 and 596 crossing the Amaziahu fault (top) and their interpretation (bottom). The 50-m-high Amaziahu escarpment is the surface expression of this spectacular listric fault which extends to a depth of 3.4 s (about 6 km). The subhorizontal portion of the fault plane probably follows the Pliocene salt layer, and the hatched areas represent possible salt pockets. Note the steeper character of the underlying basement faults and the tilted basement blocks. "B" denotes the basement reflection and N1 to N5 and S1 to S4 denote sequence boundaries north and south of the Amaziahu fault, respectively. For further interpretation and correlation of sequence boundaries see the text.

is suggested here for the Iddan fault, starting from the intersection of the fault in line 7013, passing through its intersection in line 4019, and continuing south of the southern end of line 4022. Iddan fault appears on line 4019 (Figure 5) to be dipping about 60°-70° and to have had normal sense of motion. The same fault, observed on line 7013, is far more complex, and the lower part of the sedimentary infill is gently folded. This complexity may be attributed to either a change of dip of the fault plane with depth due to the presence of salt above reflector B or to the location of the line at the intersection between the Iddan fault and the western longitudinal fault. In the absence of more subsurface data in this locality the above suggestions cannot be substantiated.

Only one seismic line (line 633, Figure 6) crosses Boqeq fault [Z. Ben Avraham et al., Transverse faults at the northern end of the southern basin of the Dead Sea graben, submitted to *Tectonophysics*, 1988]. While previous interpretation attributed the deformed area in Figure 6 (which we interpret as the Boqeq fault) to a buried salt diapir [Arbenz, 1984; E. Kashai, oral communication, 1987, D. Neev, oral communication, 1988], comparison with seismic lines crossing Mount Sedom diapir (line 632, Figure 7; lines 7003, 7020 not shown, and Kashai and Crocker, [1987, Figure 7]) shows completely different geometry of reflectors. Reflections terminating against Mount Sedom diapir are dragged up along the entire depth of the diapir and the area of the diapir itself is characterized by incoherent returns (e.g., Figure 7). Reflections terminating against the deformed area in Figure 6 are, in contrast, hardly dragged, and short segments of coherent reflections are observed down to a depth of 3 s within the deformed zone. A negative "flower"structure geometry similar in appearance to the one observed in the deformed area is shown by Harding [1983] in other locations and is interpreted by him as a strike-slip fault. We thus interpret the deformed area on Figure 6 as a fault having strike slip possibly mixed with dip slip. The orientation of the Boqeq fault cannot be determined by a single profile, but bathymetric and single-channel seismic data in the area appear to delineate a NW-SE zone of deformation (Z. Ben Avraham et al., Transverse faults at the northern end of the southern basin of the Dead Sea graben, submitted to *Tectonophysics*, 1988]. Furthermore, the lack of evidence for a fault on line 196 (see Figure 2 for

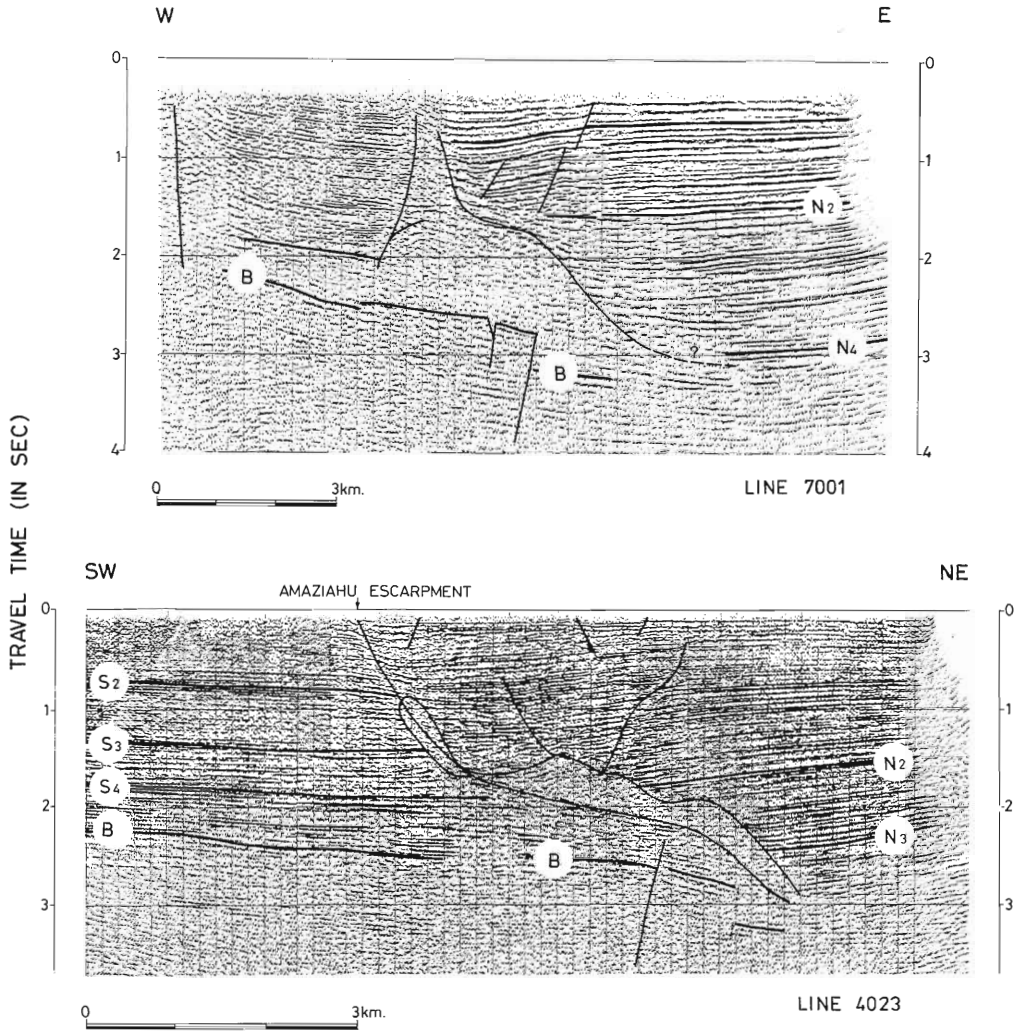

Fig. 4. Migrated seismic lines 7001 (top) and 4023 (bottom) which cross the Amaziahu listric fault at different orientations (Figure 2). The thick section of incoherent reflections around the fault probably contains mobilized Pliocene salt. Note on line 7001 that the western part of the basin (west of both the listric and the basement faults) is tilted eastward, while the central part (east of the Amaziahu fault) is subhorizontal. The annotation of reflections (B, N4 to N2, and S4 to S2) is similar to Figure 3.

location) indicates that the Boqeq fault is not part of the western longitudinal fault. We therefore suggest that the Boqeq fault is a transverse fault.

Longitudinal Faults

Two distinct depth levels are observed along E-W cross sections of the DSB. The shallower level (named "median step block" by Kashai and Crocker, [1987]) extends to a maximum depth of 3500 m (Amiaz borehole, see Figure 2 for location), while the depth of the deeper level approaches a maximum depth of 4 s (6000-8000 m) (line 7001, Figure 4). A subvertical fault separates the sedimentary infill at these two depth levels and also offsets the basement (Figures 4 and 9). Some small basement blocks are tilted and rotated eastward into the deep part of the DSB resulting in an apparent reverse faulting.

A several hundred meters escarpment and a series of normal faults comprise the western boundary of the DSB, which is also the western limit of the median step blocks. Comparison between E-W seismic lines (lines 7001, 7013, and 7014 in Figures 4, 5, and 8, and 7002 not shown) shows that the vertical throw along this boundary appears to be larger northward where the basin is the deepest (Figure 9).

The Sedimentary Fill

A marked difference between the marginal blocks (median step level) and the deep level is observed in the sediment infill

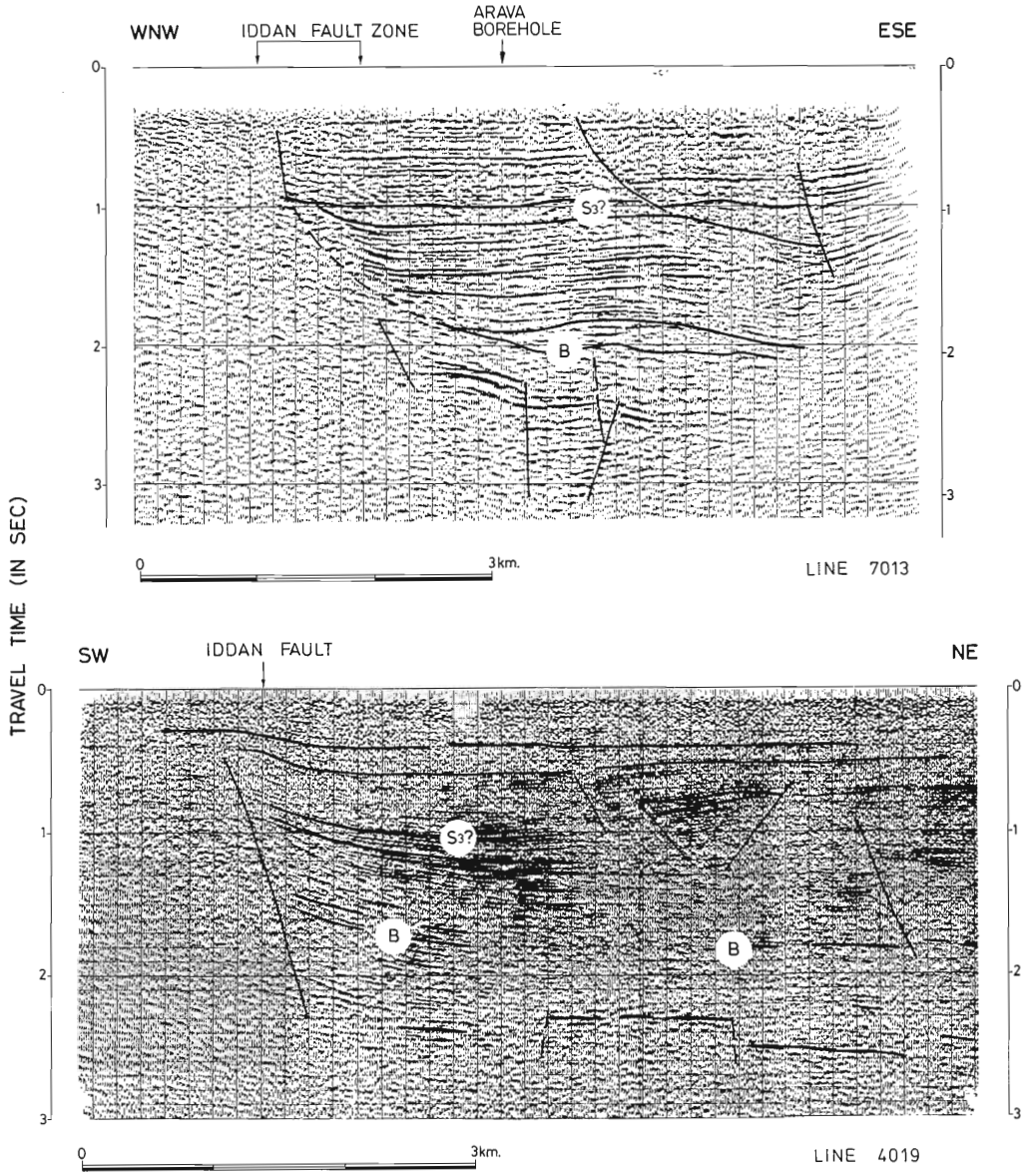

Fig. 5. Migrated seismic lines 7013 (top) and 4019 (bottom) which cross the Iddan fault, which is the southern boundary of the DSB. Note the abrupt termination of the basin fill against the surrounding basement which is acoustically opaque. The annotation of reflections is similar to Figure 3.

(Figures 4, 8, and 9). Reflections in the central deeper level are horizontal to subhorizontal (e.g. line 7001, Figure 4) whereas reflections in the median step block are tilted toward the east, that is, toward the basin. Published bathymetry and single-channel seismic data in the northern subaqueous part of the basin (lines 5 and 6 in the paper by Neev and Hall, [1979]) show a similar difference between the two levels, namely, tilted lake bottom and subsurface layers in the median step block and flat lake bottom and subsurface layers in the deep part.

The basement of the DSB appears in a N-S cross section to be gently tilted (<6°) northward (Figure 10). The sedimentary fill thickens from the Iddan fault northward by only 0.5 s and appears to hardly thicken north of Amaziahu fault. It is striking that despite the large vertical offsets observed in the DSB, the intervening sediments between the faults are relatively undeformed. Apart from the deformation associated with the transverse and longitudinal faults, only few and gentle folds and synclines (e.g., line 7013, Figure 5; Figure 6) are observed. The only exception to the lack of internal deformation is a region of a few square kilometers lying about 5 km north of Iddan fault (Figure 10). This region

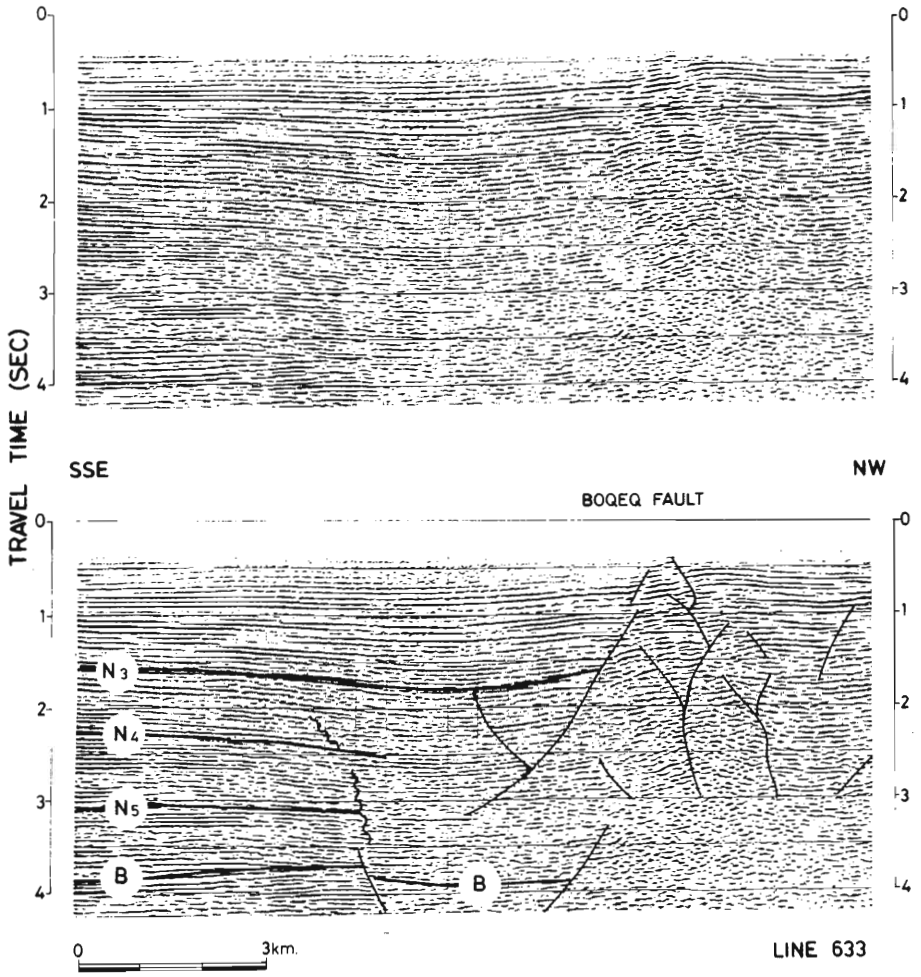

Fig. 6. Migrated seismic line 633 (top) and its interpretation (bottom). The negative "flower" structure geometry is interpreted as the Boqeq transverse fault with mixed strike slip and a dip slip. The annotation of reflections is similar to Figure 3.

is characterized by closely spaced listric faults with short vertical span within the sedimentary section. It is unclear from the seismic data whether and how much the underlying basement is faulted there.

NORTHWARD MIGRATION OF ACTIVITY ALONG THE DEAD SEA BASIN

Correlations

The time of motion along the transverse faults can be deduced from the seismic records by observing the stratigraphic patterns adjacent to the faults and by making assumptions regarding the correlation of sedimentary sequences across these faults. Before discussing this topic we outline the assumptions used in the stratigraphic analysis. The basic unit for stratigraphic analysis is the depositional sequence [Mitchum et al., 1977]. A sequence represents a genetic unit that was deposited during a single episodic event, such as the rise of DSB lake level or the rapid basin subsidence, and the boundaries separating these sequences are defined by a discordant relationship between sequences along part or all of their interface [Mitchum et al., 1977]. Furthermore, seismic reflectors tend to parallel stratification surfaces rather than the boundaries of lithologic units [Vail et al., 1977]; for instance, reflections are continuous between Melech Sedom and Amaziahu boreholes in the DSB (see Figure 2 for location) despite the marked difference between the lithologies of these two wells (E. Kashai, oral communication, 1987). Correlating sequence boundaries across fault zones in the DSB is difficult because of varying types of seismic sources and acquisition configurations between lines. In addition, key boreholes, which could help in the correlation, penetrate only the upper third of the sedimentary section and do not have reliable age dating for the recovered sediments. The following boundaries were correlated throughout the southern part of the DSB.

The undulating boundary B lies at the bottom of a stack

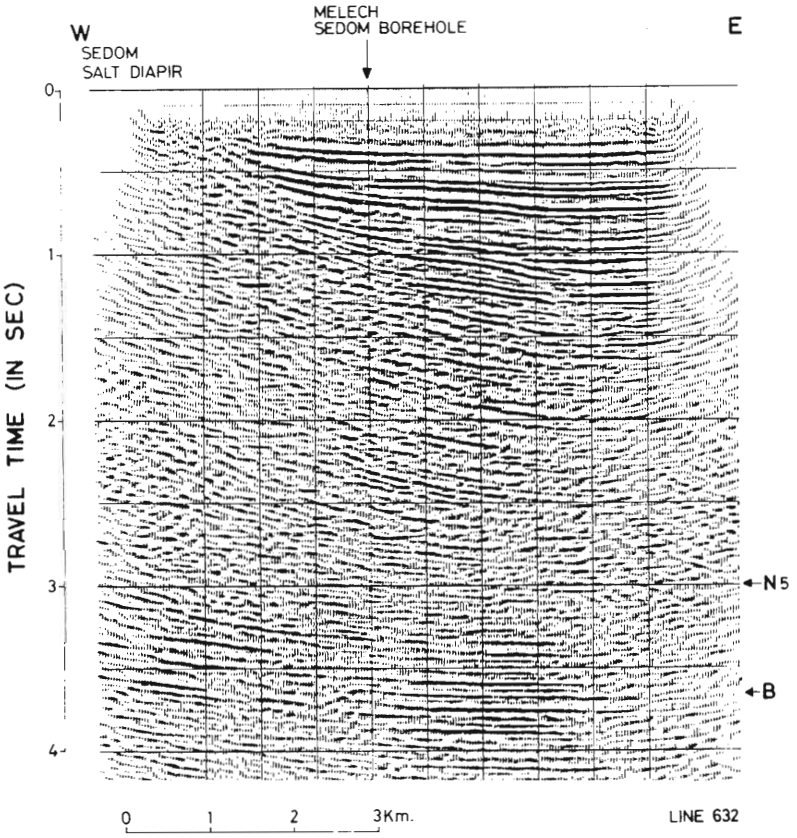

Fig. 7. Migrated seismic line 632 showing the sedimentary fill terminating against the eastern edge of Mount Sedom diapir. Note the opacity of the diapir to reflected energy and the drag of the sedimentary fill by the diapir. Basement reflections (B) are continuous under the diapir.

of reflections (e.g., line 4023 in Figure 4) and is often overlain by base-lapping reflectors (e.g. , Figure 6). Coherent reflections are occasionally observed below this horizon and are thought to represent the pre-rift sedimentary sequence (e.g., line 7013, Figure 5). Boundary B probably represents an irregular erosional surface at the base of the sediment infill , which in the DSB started in the Pliocene. We cannot, however, preclude the possibility that in places boundary B lies within or at the base of the Miocene Hazeva Formation. Following the interpretation of Kashai and Crocker [1987], boundary N5 north of the Amaziahu escarpment (e.g. Figure 3) represents the top of the evaporitic Sedom Formation because it is the lowermost reflector deformed by the rising Sedom diapir (Figure 7, see also Kashai and Crocker [1987, Figure 7]).

Sequence boundary S4 south of the Amaziahu escarpment (Figures 3 and 4) terminates in a complex zone of deformation about 5 km north of the Iddan fault (Figure 10) and is the first major unconformity above boundary B. The thickness of the sequence bounded by boundaries B and S4 is similar to the sequence, bounded by boundaries B and N5, north of Amaziahu fault. Since, as discussed below, the Amaziahu fault was not active prior to N4 time, we interpret sequence boundary S4 as the equivalent to sequence boundary N5. Similarly, boundary S2 is tentatively correlated with boundary N4 because they lie at similar thicknesses (in travel time) above boundary B and above boundaries S4 and N5. The equivalent for boundary S3 could not be identified north of the Amaziahu Fault.

Our suggestion that activity along the faults migrated northward with time, which will be developed in the next section, rests on the correct correlation of sequence boundaries across the Amaziahu fault. It is therefore necessary to independently verify the correlation between N4 and S2, the time of initiation of activity on the fault. Figure 11 shows areal balancing with a constant heave [Gibbs, 1983], applied to the cross section of Figure 3. The seismic cross section was converted to depth using a constant average velocity of 3.15 km/s. The use of constant velocity is justified by the slow increase in average velocity (V) with travel time (t) (approximately $V(t)=2.8$ km/s $+0.156*t$) documented in the Melech Sedom borehole (see Figure 2 for location). Areal balancing techniques assume that any cross sectional area created during basin formation must be accounted for elsewhere in the geologic interpretation [Bosworth and Gibbs, 1985]. These techniques are commonly used to determine the depth to the listric fault detachment. The unknown in the case of the Amaziahu fault is the correlation between N4 and S2, whereas the depth of the detachment is observed. The cross sectional

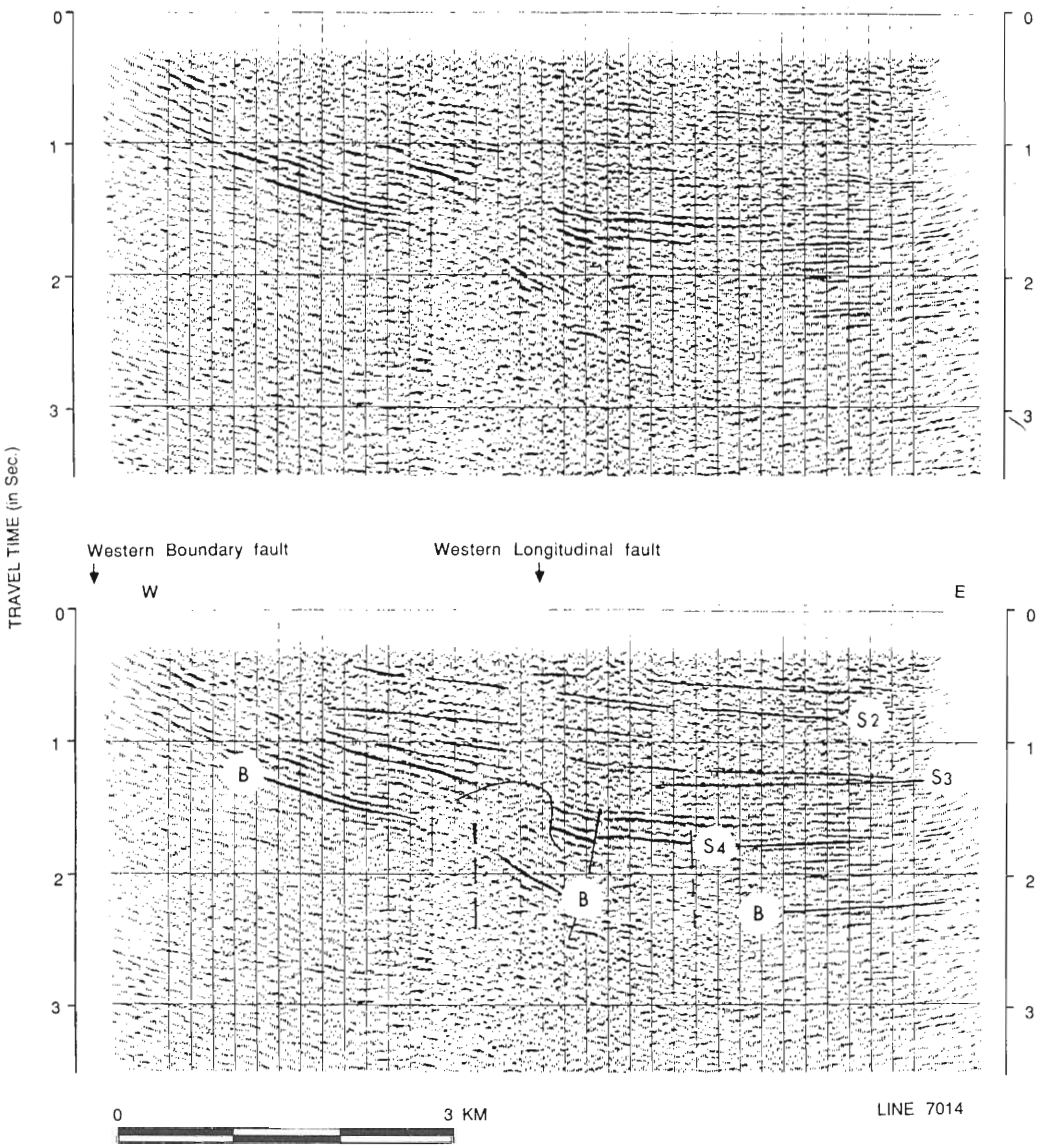

Fig. 8. Migrated seismic line 7014 (top) and its interpretation (bottom). This line intersects the western longitudinal fault south of the Amaziahu escarpment. Note that below S3 and west of the longitudinal fault both the basement and infill are tilted eastward, while east of the longitudinal fault they are subhorizontal. Above S3 the basin fill is sagging without a noticeable offset along the western longitudinal fault.

area between the listric fault and the northward continuation of S2 (hatched area A in Figure 11) must be equal to the product of the net crustal extension ($\varepsilon_{s1}+\varepsilon_{s2}=\varepsilon_s$) times the depth of the detachment (D=N4-B). However, since part of the newly formed cross sectional area is due to subsidence of the underlying basement, the amount of basement subsidence should be subtracted from the total new area (dotted area A' in Figure 11). The difference between area A and area A' should then be equal to the area B (ε_s x D) if the geometry of the fault and the correlation between S2 and N4 are properly identified. Area A minus area A' is only 10% larger than area B, which implies that the balancing of the cross section is correct and therefore confirms the correlation between S2 and N4 across the Amaziahu fault.

Timing of Activity Along the Faults

The initiation of motion on the Amaziahu listric fault is indicated by the thickening of the N4-N3 sequence into the fault. The divergent pattern of the reflectors within sequence N4-N3 (Figure 3) was presumably caused by deposition while rotation down the listric fault was taking place. The 1.0-s-

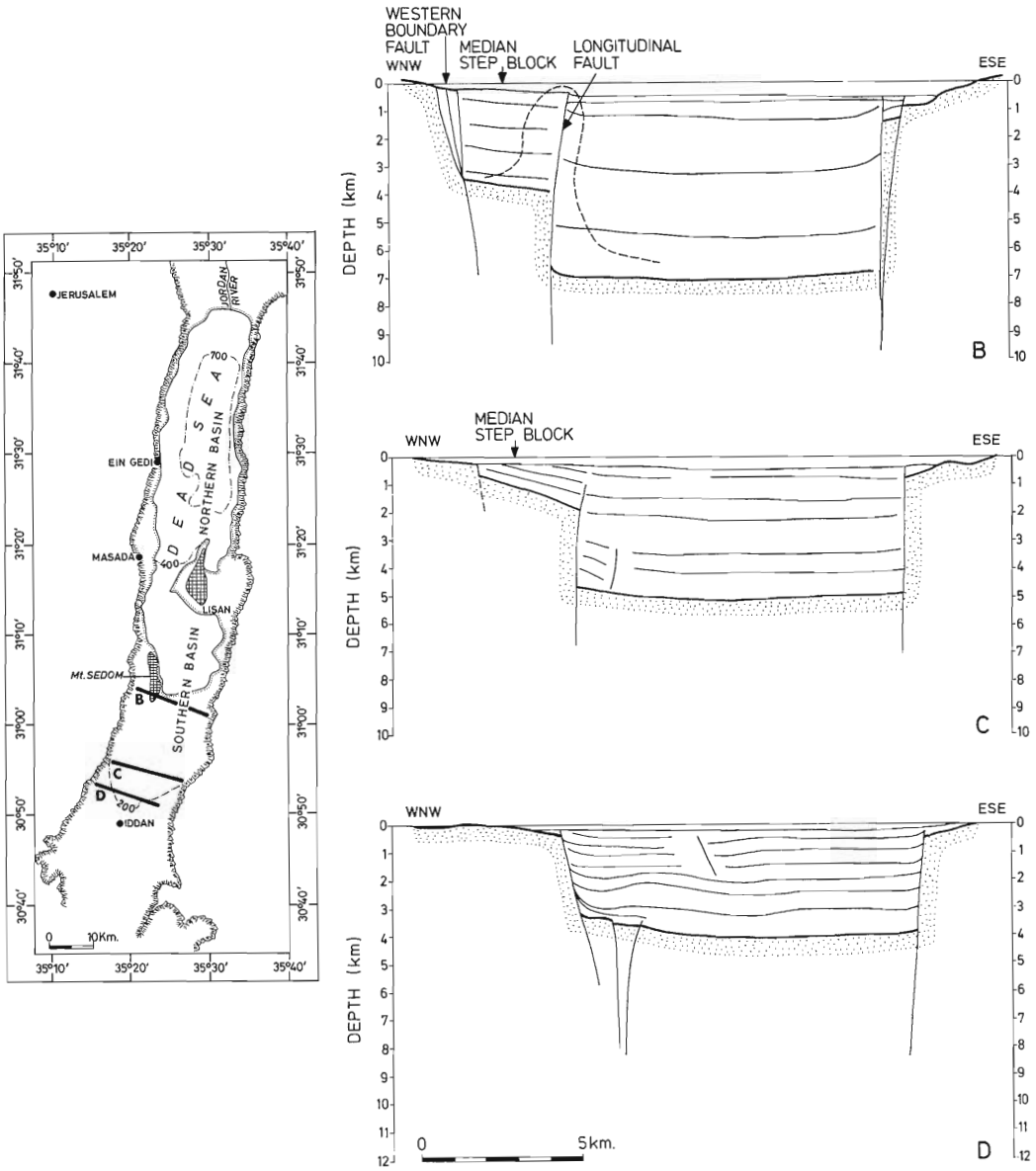

Fig. 9. Schematic line drawings showing three E-W cross sections of the basin (right) and their location in a map view (left). The top cross section is based on seismic lines 7001, 595, and 7002, the middle one on line 7014, and the lower one is based on line 7013. The basement is shaded. The approximate depth scale is based on the conversion of travel times to depth using a uniform acoustic velocity of 3.5 km/s. The eastern part of the cross sections is extrapolated due to a lack of subsurface coverage. The dashed line in the top cross section marks the location of Mount Sedom diapir. The succession of cross sections suggests that the western part of the basin (the "median step block") deepens and tilts eastward as the main part of the basin subsides. The fault separating the main part of the basin from the western part is also tilted eastward resulting in an apparent reverse motion on the fault.

thick sequence N5-N4, characterized by constant thickness and by reflectors paralleling each other, was deposited before the inception of faulting. This sequence amounts to about one-third the total thickness of Pleistocene sediments (in travel time) because N5 corresponds to the boundary between the Pliocene salt and the Pleistocene. Hence the Amaziahu fault probably dates from the lower to middle Pleistocene.

Thickening of the sequence N2-N1 toward the fault indicates that activity on the fault has continued intermittently throughout the Pleistocene. The 50-m-high surface escarpment indicates that the Amaziahu fault has also been active in the recent past. The geographical proximity of the basement offsets and the Amaziahu listric fault (Figures 3 and 4) suggests that basement faulting was coincidental with the

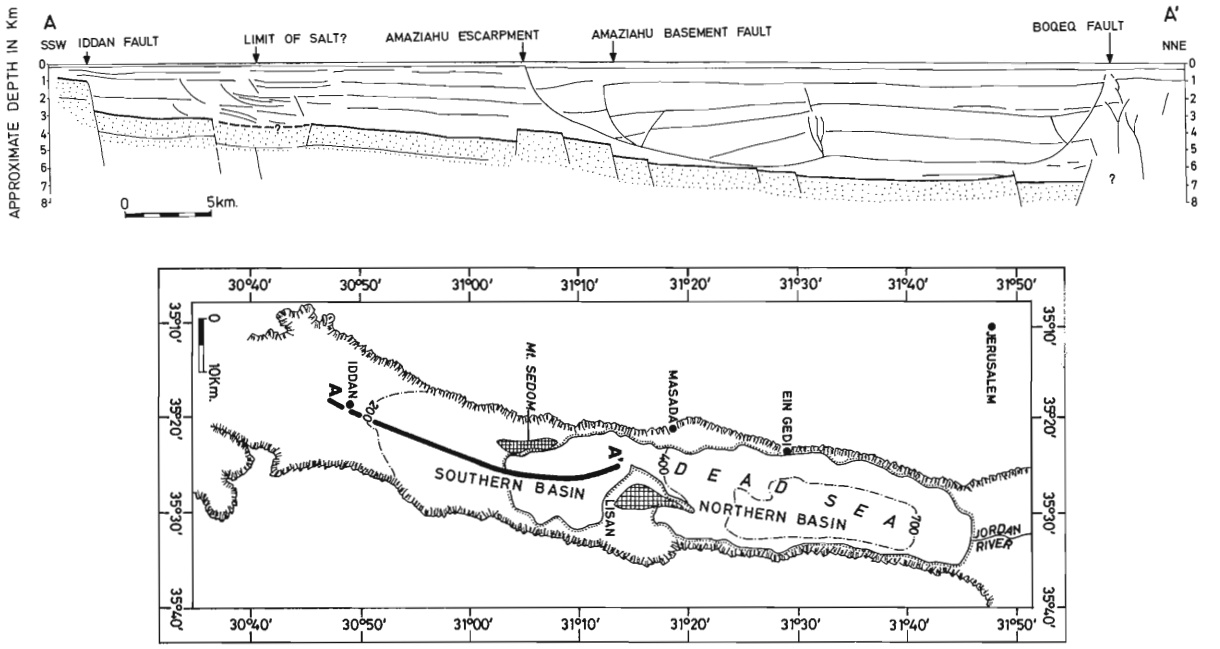

Fig. 10. (top) Line drawing of seismic lines 4022, 596, and 633 showing our interpretation of the structure along the long axis of the basin. (bottom) Location of the line drawing. The basement is shaded. The approximate depth scale is based on the conversion of travel times to depth using a uniform acoustic velocity of 3.5 km/s. The main deepening of the basin to the north occurs at the Iddan and Amaziahu traverse faults while the basement between them is gently dipping to the north. Despite the large vertical movement of the basement the layers of sedimentary infill are only mildly perturbed.

initiation of the listric fault. In particular, the thickest part of the divergent sequence N4-N3 and a secondary buried ancient (?) trace of a listric fault are located above the largest basement offset (Figures 3 and 11).

The timing of activity on Iddan fault to the south is indicated by the wedging out of the reflectors toward the fault zone in the interval between 1.1-1.5 s (between boundaries B and S3?) in line 4019 and between 1.45-1.55 s in line 7013 (Figure 5). A later short phase of activity is implied by the drag of the overlying reflectors on the fault seen in line 4019 (0.9-0.6 s). The Iddan fault has not been active in the recent past (above 0.6 s in line 4019, Figure 5) as is indicated by the lack of geological markers at the surface. Provided that we correctly extended the correlation between N5 and S4 and between N4 and S2 to the southern end of the basin, then the activity on Iddan fault started during the early period of deposition of the Amora formation (early Pleistocene?) before the Amaziahu fault was formed.

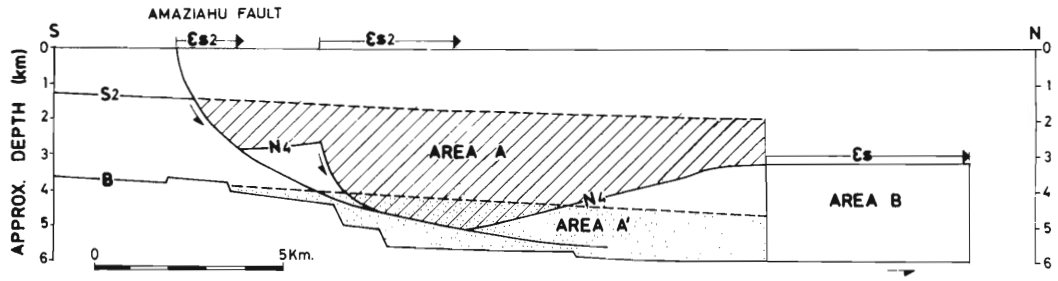

Fig. 11. A balanced cross section [Gibbs, 1983; Bosworth and Gibbs, 1985] of the seismic profile of the Amaziahu listric normal fault (Figure 3). In a properly balanced cross section the space created by the movement along the listric fault (area A) must equal the sum of extensions along the fault, $\varepsilon s1+\varepsilon s2=\varepsilon s$, multiplied by the depth to the structural compensation D, where D equel the interval between N4 and B. In other words, area A - area A' = area B where area B = εs x D. It is necessary to subtract from area A that part of the cross-sectional space which was created by basement faults (area A') and not by the Amaziahu listric fault. The dashed lines represent the linearly extrapolated prelistric and prebasement faulting surfaces S2 and B. See text for further explanation.

Tectonic activity along the western longitudinal fault between the Iddan and the Amaziahu faults also appears to be confined to the early part of basin deposition (line 7014, Figure 8). Whereas the B-S4 sequence and part of the overlying S4-S3 sequence are faulted and vertically offset, the reflections above 1.3-1.5 s sag into the center of the basin and onlap against the tilted median step block (Figure 8). In addition, a gradual northward thickening of the shallow sequence (above S2) toward the Amaziahu escarpment is observed on the N-S oriented seismic lines (e.g., line 4023, Figure 4; Figure 10). The observed onlap and the gradual thickening of the shallow sections between the Iddan and Amaziahu faults indicate a recent sagging of the southern segment of the DSB toward the north and the east.

Initiation of activity along the Boqeq fault north of the Amaziahu fault probably does not predate time N3 because the underlying reflections are uniformly folded to form a gentle syncline south of the fault zone (Figure 6). The syncline, however, is filled with fairly horizontal reflectors which onlap on sequence boundary N3, suggesting a fairly short period of activity at that time. The vertical offsets seen in the shallowest part of the fault zone (< 1.5 s) and the warping of reflectors adjacent to the fault zone indicate an additional recent phase of activity.

Comparison of the time of activity in the three transverse faults indicates the possibility that the initiation of activity advanced northward with time. Activity began at the southern boundary of the DSB, the Iddan fault, in the early (?) Pleistocene and was followed in the Early to middle (?) Pleistocene (N4-N3) by the creation of Amaziahu fault. The movement along the Boqeq fault, further to the north, did not start until time N3 (middle(?) Pleistocene). Activity along the Iddan fault and the western longitudinal fault south of the Amaziahu fault terminated during the middle to late(?) Pleistocene, and the southernmost segment of the DSB between Iddan and Amaziahu faults has since been gently sagging northward and eastward.

DISCUSSION

The Internal Structure of the Dead Sea Basin

Our interpretation of the three-dimensional structure of the DSB is illustrated in a map view (Figure 12) and in a longitudinal (Figure 10) and three latitudinal (Figure 9) cross sections. The cross sections are based on the multichannel seismic data analyzed in this study, but the map includes additional data compiled from other sources (single channel seismic survey [Neev and Hall, 1979], land geology [Arkin et al., 1981; Bentor et al., 1965; Gilat and Agnon, 1981; Picard and Golani, 1965; Raz, 1986; Rot, 1970], the magnetic field, [Frieslander and Ben-Avraham, 1989], and the gravity field, unpublished files). The structure is characterized by the following aspects.

Despite the large known vertical offsets, deformation in the southern part of the DSB takes place mainly on the transverse and longitudinal faults, and the intervening sediments are relatively undeformed (Figures 9 and 10). E-W cross sections of both the northern and the southern subbasins show a full-graben geometry of flat horizontal strata of sediment infill. We assume a full-graben geometry although

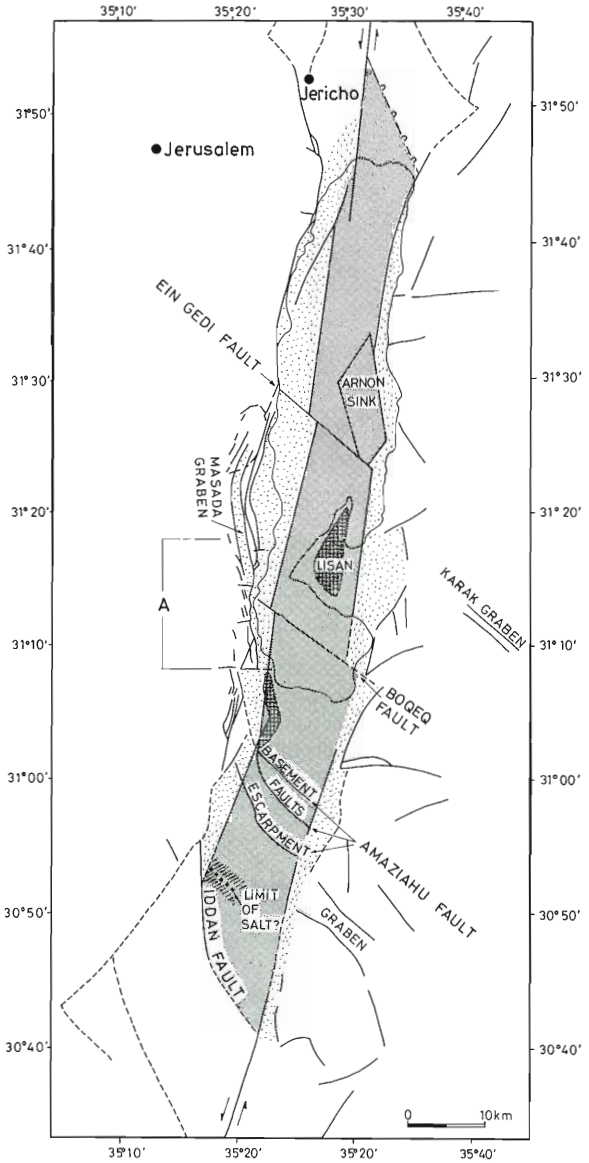

Fig. 12. A map showing our interpretation of the structural elements of the DSB. The shaded area which represents the central deep part of the basin is separated from the surrounding dotted area, the marginal blocks, by the western and eastern longitudinal faults. The western margin is limited by arcuate normal faults to the west and is tilted eastward. Little is known about the structure of the eastern margin. Solid lines mark faults and dashed lines their extrapolations. Faults are modified within the northern part of the basin [from Neev and Hall, 1979] and along the boundaries [from Bentor et al., 1965; Gilat and Agnon, 1981; Picard and Golani, 1965; Raz, 1986; Rot, 1970]. The shape of the Arnon sink, a subsurface depocenter, is simplified [from Neev and Hall, 1979]. The area marked by A west of the Boqeq fault contains several strike-slip faults [Arkin et al., 1981]. Our suggestion for the location of the northern boundary fault of the basin is marked by question marks.

we have no information about the easternmost part of the graben. However, a complete cross section of the northern basin (e.g., lines 5 and 6 in the paper by Neev and Hall [1979]) justifies this assumption. There is only one exceptional area, named the Arnon Sink (see Figure 12), in which localized differential subsidence has occurred [Neev and Hall, 1979]. Seismic observations in the Elat Deep in the Gulf of Aqaba (Elat), another pull-apart basin along the Dead Sea strike-slip fault system, shows by way of contrast a half-graben geometry tilted to the east [e.g., Ben-Avraham, 1985, Figures 5 and 6]. The southernmost segment of the DSB (south of the Amaziahu fault) is gently tilted northward, but the rest of both the southern and the northern subbasins are horizontal along their long axis. We thus conclude that, in general, sediments in the DSB are deposited horizontally and undergo little subsequent deformation. We attribute the horizontal sediment deposition to a lacustrine depositional environment which prevailed during much of the evolution of the DSB [Neev and Emery, 1967; Kashai, 1989], but the lack of internal deformation characterizes the tectonic style of deformation.

The southern part of the basin is divided into equidistant segments, 20-30 km long and 7-10 km wide, which are bounded by transverse faults (Figure 9, 10, and 12). This division can be also extended northward to include the Lisan segment because a fourth diagonal fault, the Ein Gedi fault [Neev and Hall, 1979], is located about 25 km north of the Boqeq fault (Figure 12). The Ein Gedi fault is defined by a pronounced bathymetric escarpment [Neev and Hall, 1979] and a steep horizontal gradient of the magnetic field (Frieslander and Ben-Avraham, 1989). The northern part of the DSB, north of Ein Gedi fault, is 50 km long, and a transverse fault cutting it in half was not identified.

Although it has a large vertical offset, the western longitudinal fault appears subvertical in the seismic data. A bathymetric map of the northern subbasin indicates that the surficial trace of the western boundary fault is straight and that it is aligned with the southern termination of the Dead Sea strike-slip strand in the Jericho area north of the DSB [Neev and Hall, 1979]. Various authors [Neev and Hall, 1979; Garfunkel, 1981; Kashai and Crocker, 1987] have suggested that the western longitudinal fault in the northern subbasin is part of the Dead Sea strike-slip system. The subvertical western longitudinal fault in the southern part of the DSB has probably also originated as a strike-slip fault. Our map (Figure 12) suggests that the surficial trace of the western longitudinal fault is discontinuous where it intersects the transverse faults. Such a straight but discontinuous trace is expected since the long axis of the DSB gradually changes from NE to NNE. This implies that individual segments within the basin undergo small amounts of rigid block rotation and that a component of strike slip should be detected on the transverse faults bounding them. The Boqeq fault underwent a strike-slip motion, but movement along the Amaziahu and the Iddan faults appears to be normal, although a strike-slip component along these faults cannot be ruled out on the basis of seismic data alone.

The western margin of the DSB is only half as deep (or less) as the main part of the basin and is separated from it by the western longitudinal fault. Unlike the flat horizontal sediments filling the deeper part of the basin, the sediments filling the western margin (and the underlying basement) are tilted eastward by as much as 24° (Figure 8, assuming an average sediment velocity of 3.15 km/s). The depth of the western margin appears to increase with increasing depth of the central part of the basin. The western longitudinal fault within the basement of some seismic lines (e.g., line 7001, Figure 4) appears to have had a reverse motion. The tilt, the deepening, and the apparent reverse motion suggest that the western margin has collapsed and rotated into the basin as a result of deepening of the DSB eastward of the western longitudinal fault. Hence it appears that the DSB has widened with time by an asymmetric subsidence of the western margin. Masada Graben and tension cracks on the cliffs overlooking the Dead Sea depression [Arkin et al., 1981](see Figure 12 for location) are interpreted as the current manifestation of basin widening. The western boundary of the DSB is a normal fault with an arcuate surficial trace [Bentor et al., 1965; Gilat and Agnon, 1981; Picard and Golani, 1965; Raz, 1986; Rot, 1970]. Subsurface data, summarized in Figure 9, and previous geologic inference [Zak and Freund, 1981] suggest that the vertical throw across the western boundary amounts to several kilometers . Little is known about the eastern margin of the DSB and whether its structure is similar to that of the western margin. Single-channel seismic lines in the northern subaqueous part of the basin show a pronounced steep escarpment and a large vertical throw which were interpreted as the eastern longitudinal fault [Neev and Hall, 1979]. The trace of the eastern longitudinal fault across the Lisan is defined by a steep horizontal gradient in the Bouguer gravity anomaly field [Bender, 1968]. Evidence for the continuation of the fault south of the Lisan is lacking but Kashai and Crocker [1987] have extended the eastern longitudinal fault northward from the southern strand of the Dead Sea strike-slip fault in the Arava valley (see Figure 12).

Using correlation with drill holes, the Pliocene salt layer (Sedom Formation) was interpreted in seismic lines to underlie the Pleistocene sedimentary infill in the vicinity of the Mount Sedom diapir (Ginzburg and Kashai [1981], Kashai and Crocker [1987], and the sequence B-N5 in this study). Earlier in the paper we correlated the sequence B-N5 north of the Amaziahu fault with the sequence B-S4 south of the fault. The southern termination of the salt layer is probably located at the zone of internal deformation north of Iddan fault (Figure 10 and 12) because basement becomes shallower (by 0.2 s) there, boundary S4 cannot be traced south of this zone, and there is no evidence for salt along the Iddan fault plane (line 4019, Figure 5). A salt layer may also underlie the entire northern subbasin [Neev and Hall, 1979]. In addition, salt is also rising along some transverse and longitudinal fault planes in the southern subbasin (Figures 3, 4, 8 and line 7002, not shown) and along the western longitudinal fault in the northern subbasin (small subsurface diapirs in the paper by Neev and Hall, [1979]). Thus it appears that salt underlies and surrounds much of the sedimentary infill in the deep level of the DSB. The lack of any significant internal deformation within the sedimentary infill (apart from the transverse faults) may be explained by the low shear strength of the salt which acts to decouple the infill from the tectonic movements of the basement and the surrounding walls.

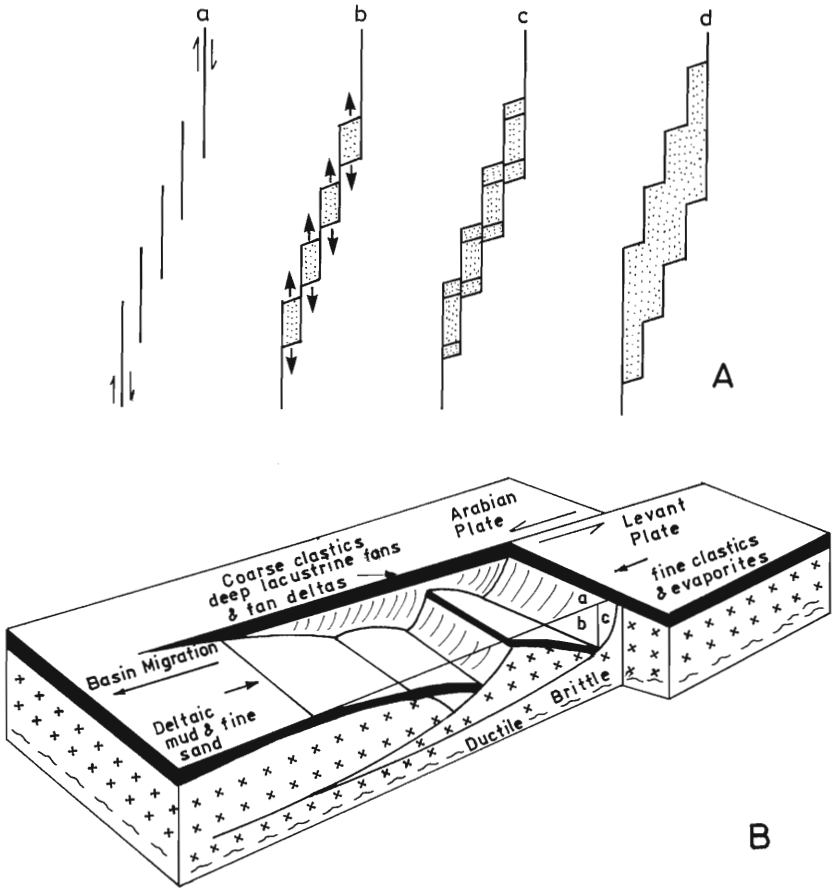

Fig. 13. Current conceptual models for the development of pull-apart basins: (a) A series of depressions are formed and enlarged with time (a and b) as blocks across a series of en echelon oversteps move in opposite directions. The depressions ultimately coalesce to form a large basin (c and d), and the relics of the oversteps are preserved as transverse faults within the basin [after Aydin and Nur, 1982]. (b) An asymmetric N-S extension along a midcrustal detachment creates a gentle flexure of the northern boundary of the basin and a southward tilt of the basement and sedimentary fill (after Arbenz [1984] and modified by Manspeizer [1985]). Neither of these models is supported by the observations of the present study.

Analysis of deformation within the sedimentary infill is therefore not necessarily indicative of the structure of the basement, as seen, for example, in the different styles of deformation of the basement and of the sedimentary fill in the Amaziahu fault (Figure 3). The amount of horizontal extension of the sedimentary fill across the Amaziahu fault is 5.4 km (Figure 11), while the underlying basement has been extended by up to only 1-1.5 km (assuming normal faults with a dip of 67°). The discrepancy between the amounts of extension in the basement and in the sedimentary infill can be settled either by an additional basement extension somewhere else along the basin or by compression of the sedimentary sequence. The second option is the more likely one as there are large salt diapirs in this part of the basin (Mount Sedom and Lisan diapirs, see Figure 12 for location). Mount Sedom diapir has roughly the dimensions of 12 x 3 x 5 km or 180 km^3. Assuming that area B (Figure 11) represents the average displaced material along the 15-km-long Amaziahu fault, we have 15 km x (5.4 km) x 2.8 km or 227 km^3. Thus the space problem introduced by the excess extension of the sedimentary fill can be solved to a large extent by the continuous escape of salt through Mount Sedom diapir. This suggests a possible genetic relationship between the activity of Amaziahu fault and the uplift of the Mount Sedom diapir.

The Evolution of the Dead Sea Basin

The DSB is often cited as a type example of a pull-apart basin [e.g. Aydin and Nur, 1982]. Pull-apart basins develop along wrench faults with releasing bends, releasing fault junction, or releasing fault overstep [Harding et al., 1985]. A depression is formed and enlarged when the blocks across a bend or an overstep move in opposite directions [Mann et al., 1983]. The DSB is envisioned as a pull-apart basin between left-stepping en echelon faults (releasing fault overstep) (Figure 13a) in the left-lateral Dead Sea strike-slip system

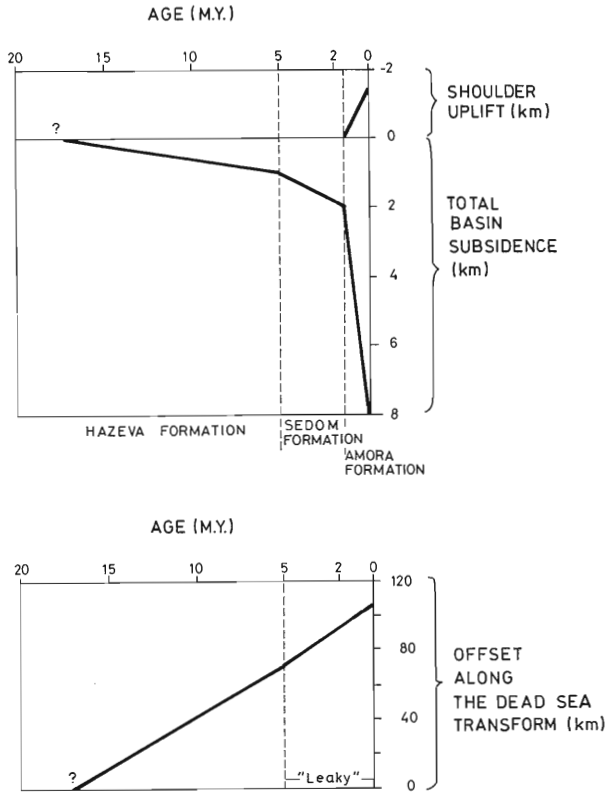

Fig. 14. An illustration of the temporal relationship between several tectonic events in the vicinity of the DSB. Movements are linearly interpolated between ages at which their magnitudes can be estimated. Estimates for the total subsidence of the basin with time (top) are based on the stratigraphic interpretation of the seismic lines (see text). Estimates for total uplift (top) are based on the current elevation of Late Cretaceous layers east of the DSB. The cumulative displacement along the Dead Sea strike-slip fault system(bottom) is from Joffe and Garfunkel [1987], who assumed a small component of extension perpendicular to the strike-slip system ("leaky") during the Plio-Pleistocene.

[Quennell, 1959; Freund and Garfunkel, 1976]. The longitudinal faults in the DSB are the continuation of the overstepping strike-slip faults, and the deep basin, bounded by these faults, is subsiding symmetrically as a full-graben. Moreover, the length of the DSB (about 110 km) is in accord with the cumulative amount of slip, 105 km, along the Dead Sea fault system [Freund et al., 1970].

A certain degree of complexity is introduced, however, to the simple pull-apart model by our observations of the temporal evolution of the DSB. The first observation concerns the age of the sedimentary infill. The relative thickness (in travel time) of sediments and the interval N5-present (Pleistocene) versus the sequence B-N5 (Pliocene) is about 3:1-4:1, which implies that rapid subsidence has occurred only since the Pleistocene (Figure 14). Although there is a possibility that the original thickness of the Pliocene salt layer was >> 1000 m, and the salt was later squeezed into diapirs, sedimentological evidence [Sa'ar, 1985] also argue for a low topographic relief during the Pliocene and a high relief during the Pleistocene. Sands within the Sedom formation (Pliocene) were mainly derived from the immediately underlying Hazeva formation (Miocene), while sands within the Amora Formation (Pleistocene) sample the entire Phanerozoic basement [Sa'ar, 1985]. Therefore a shallow depression associated with the DSB appears to have existed during the Pliocene, but the large vertical offsets, which now characterize the DSB, are limited to the Pleistocene (Figure 14). This is despite the fact that the Dead Sea strike-slip fault system has probably been active since the middle Miocene [Garfunkel et al., 1974; Steckler and ten Brink, 1986]. Garfunkel [1981] attempted to explain this temporal discrepancy by suggesting that a slight change in the relative motion between Africa and Arabia at the beginning of the Pliocene introduced a component of extension across the Dead Sea fault system (a "leaky transform fault") and initiated rapid basin subsidence. But evidence for thermal anomalies, which are expected to accompany the leaky pull-apart basin, are lacking [Ben-Avraham et al., 1978; Kashai and Crocker, 1987; Feinstein, 1987].

The second set of observations include the time of initiation of motion along the transverse faults and its apparent northward migration. The pull-apart model, based on simple geometrical considerations, predicts that transverse faults are the complementary sides of a bend or overstep across which the basin was extended (Figure 13). The existence of several transverse faults within basins is explained in this model by the coalescence of several smaller pull-apart basins [Aydin and Nur, 1982]. Our observations suggest, on the other hand, that the transverse faults within the DSB have been active only after the basin started forming and that activity commenced along the southernmost transverse fault and migrated with time to transverse faults located further north. The northward migration of activity with time on transverse faults corroborates the earlier suggestion of a northward migration of the depocenter of the DSB [Zak and Freund, 1981].

A fault defining the northern boundary of the DSB has not been found. Several authors [Arbenz, 1984; Kashai and Crocker, 1987; Reches, 1987] have consequently hypothesized that the northern boundary is a flexure that tilts beds gently toward the south. This has led Arbenz [1984] (see also Manspeizer, [1985]) to propose that the DSB was formed by north-south extension on a low-angle detachment dipping to the north and leveling off at a depth of 15 km (Figure 13b). The data, however, do not support this model. First, according to this detachment model the overlying blocks should tilt southward contrary to the tilt observed in the seismic sections south of the Amaziahu Fault (e.g., Figure 10). Second, reflections showing south dipping flexure are not observed in seismic profiles at the northern end of the lake (e.g., line C in the paper by Neev and Hall, [1979]). Reflections have a horizontal attitude at distances as small as 10 km from the northern coast of the Dead Sea. Third, the underlying basement faults, wherever identified (e.g. Figures 3, 4, and 5) seem to be high-angle faults. We suggest that a northern boundary fault zone does exist but is located in an area which

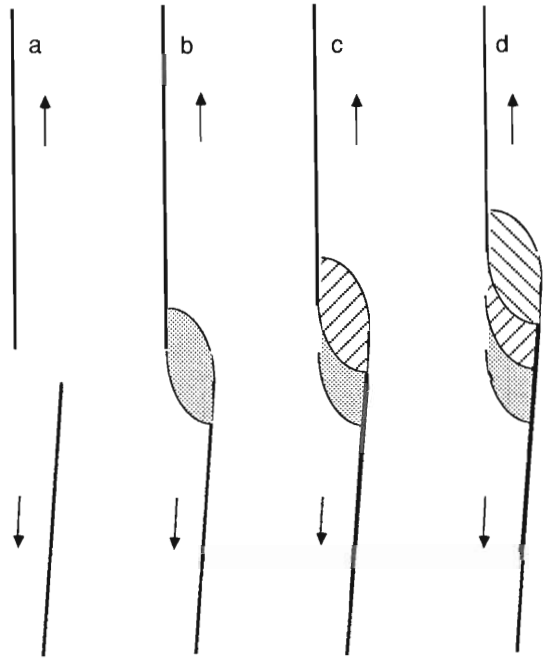

Fig. 15. A suggested scenario for the development of pull-apart basins such as the DSB. (a) Common terminations of two strands of a strike-slip fault. (b) A basin is formed between them. (c) The southern strand propagates northward with time, resulting in the gradual transfer of strike-slip motion from the southern end of the northern strand to the propagating southern strand. (d) The basin is elongated after several episodes of propagation, its depocenter has migrated northward, and new transverse faults are formed to the north while the activity along the southern transverse faults and the southern end of the northern strand is waning.

does not have subsurface coverage and which is partly covered by the delta of the Jordan river. Our suggested orientation of the northern boundary fault zone (see Figure 12) is parallel to topographic contours north of the lake and to the contours of the magnetic field in an area characterized by a steep horizontal gradient (Frieslander and Ben-Avraham, 1989).

Mechanical models for pull-apart basins have taken two approaches. The first one envisions the en echelon strike-slip faults as surfaces of discontinuity and calculates the displacement field on the basis of dislocation theory [Rodgers, 1980]. The second approach views these faults as fractures and calculates the local stress field caused by the interaction of the two fracture tips (Segall and Pollard, 1980). We do not attempt in this paper to explain the formation of the DSB by a quantitative model. We would, however, like to suggest that various physical dimensions such as the basin length and depth and the uniform spacing between transverse faults are related to the mechanical response of the crust rather than the preexisting configuration of oversteps. A possible scenario for the development of the DSB with time is shown in Figure 15. Two strands of the en-echelon fault system (Figure 15a) are reorientated in a way which allows the development of a basin between the terminations of the two strands (Figure 15b). With time the southern strand propagates northward while the northern strand retreats (Figures 15c and d) resulting in the transferring of the area enclosed by the two strands from the Arabian plate to the African plate. New transverse faults develop as this northward propagation and retardation takes place in accord with the observations in the DSB. The southern parts of the northern strand and the southernmost transverse faults become inactive at the same time, as indicated by the cessation of activity along the southern part of the western longitudinal fault and the Iddan fault. The subsidence of new portions of the basin and the cessation of activity in the southernmost part of the basin due to the propagation and retardation of the Dead Sea strands is likely to be manifested in a northward migration of the basin depocenter, as is indeed suggested by Zak and Freund [1981]. If propagation of the southern strand occurs episodically by rupture we would expect an abrupt onset of subsidence along the entire newly acquired segment of the basin in accord with the lack of internal deformation within segments and with the subhorizontal attitude of the lake bottom and the sedimentary fill in the northern subbasin of the DSB. If the rupture extends a fairly constant distance, the segments which lie between the transverse faults will have a uniform length apart from the northernmost segment which will be twice as long (Figure 15d) in accord with the observations in the DSB.

CONCLUSIONS

Using available industrial multichannel seismic reflection lines we have attempted to draw a coherent picture of the anatomy of the Dead Sea pull-apart basin. The high quality, deep penetration, and areal coverage of the data allowed the identification of fault traces as well as the correlation between reflectors in the southern part of the DSB. On the basis of these correlations we conclude that activity has migrated northward with time along newly created transverse faults while the southernmost transverse fault and the southern part of the northern strand have become inactive. In accord with these observations we have suggested a scenario for the development of the DSB in which the basin grows northward with time by the propagation of the southern strand of the Dead Sea fault and the retardation of the northern strand. The data also show that while the deeper part of the DSB subsides as a full-graben, the western margin is tilted and collapses eastward into the basin in a process which makes the basin wider with time. Observations and inference suggest that a salt layer exists under a major part of the basin floor as well as along many of the faults, effectively decoupling the sedimentary infill from the deformation of the underlying basement and making it difficult to deduce about basement deformation from the observed shallow one. Despite this difficulty we believe that the DSB constitutes one of the better examples of pull-apart basins because of its large dimensions, simple structure, and current subsidence.

Acknowledgement . We would like to thank M. Goldberg, Ministry of Energy, and J. Fisher, O.E.L. for their permission to use and publish the seismic data, and R. Asael, I. Gold, and U. Frieslander for their technical help in retrieving these data. E. Kashai has kindly provided his manuscripts

before publication. Discussions with W. Bosworth, E. Kashai, H. Ron, and G. Shamir and critical reviews by A. Aydin, T. Brocher, and G. Shamir led to many improvements in the manuscript. We are grateful to T. Harding and an anonymous reviewer for their thorough reviews and helpful suggestions. This study was supported by a grant from the Israeli Academy of Science. UtB would like to thank A. Nur for his hospitality and financial support at Stanford.

REFERENCES

Arbenz, J.K., Oil potential of the Dead Sea area, *Rep no. 84/111*, Seismica Oil Explor. Ltd., Tel Aviv, 1984.

Arkin, Y., A. Gilat, and A. Agnon, Mediterranean-Dead Sea Project: Geotechnical survey of area proposed for an underground power station, *Rep. MM/3/81*, 15 pp., Geol. Survey Isr., Jerusalem, 1981.

Aydin, A,. and A. Nur, Evolution of pull-apart basins and their scale independence, *Tectonics, 1*, 91-105, 1982.

Begin, Z.B., A. Ehrlich, and Y. Nathan, Lake Lisan, the Pleistocene precursor of the Dead Sea, *Bull. Isr. Geol. Surv., 63*, 30 pp., 1974.

Bender, F., *Geologie von Jordanien*, 230 pp., Borntraeger, Berlin, 1968.

Ben-Avraham, Z., Structural framework of the Gulf of Elat (Aqaba), northern Red Sea, *J. Geophys. Res., 90*, 703-726, 1985.

Ben-Avraham, Z., R. Hanel, and H. Villinger, Heat flow through the Dead Sea rift, *Mar. Geol., 28*, 253-269, 1978.

Bentor, Y.K., A. Vroman, and I. Zak, Geological map of Israel, scale 1:250,000, southern sheet, Govt. Printer, Jerusalem, 1965.

Bosworth, W. and A.D. Gibbs, Discussion on the structural evolution of extensional basin margins, *J. Geol. Soc. London, 142*, 939-942, 1985.

Crowell, J.C., Sedimentation along the San Andreas fault, California, in *Modern and Ancient Geosynclinal Sedimentation, Publ. 19*, edited by R.H. Dott, Jr. and R.H. Shaver, pp. 292-303, Society of Economic Paleontologists and Minerologists, Tulsa, Okla., 1974.

Eyal, Y., M. Eyal, Y. Bartov, G. Steinitz, and Y. Folkman, The origin of the Bir Zreir rhomb-shaped graben, eastern Sinai, *Tectonics, 5*, 267-277, 1986.

Feinstein, S., Constraints on the thermal history of the Dead Sea graben as revealed by coal ranks in deep boreholes, *Tectonophysics, 141*, 135-150, 1987.

Freund, R., Kinematics of transform and transcurrent faults, *Tectonophysics, 21*, 93-134, 1974.

Freund, R., Z. Garfunkel, I. Zak, M. Goldberg, B. Derin and T. Weissbrod, The shear along the Dead Sea rift, *Philos. Trans. R. Soc. London Ser. A, 267*, 107-130, 1970.

Freund, R., and Z. Garfunkel, Guidebook to the Dead Sea rift, 27 pp., The Hebrew University, Jerusalem, 1976.

Frieslander, U. and Z. Ben-Avraham, The magnetic field over the Dead Sea and its vicinity, *Mar. Pet.. Geol.*, in press, 1989.

Garfunkel, Z., Internal structure of the Dead Sea leaky transform (rift) in relation to plate kinematics, *Tectonophysics, 80*, 81-108, 1981.

Garfunkel, Z., and A. Horowitz, The upper Tertiary and Quaternary morphology of the Negev, Israel, *Isr. J. Earth Sci., 15*, 101-117, 1966.

Garfunkel, Z., Y. Bartov, Y. Eyal, and G. Steinitz, Raham Conglomerate- New evidence for Neogene tectonism in the southern part of the Dead Sea Rift, *Geol. Mag., 11*, 55-64, 1974.

Garfunkel, Z., I. Zak, and R. Freund, Active faulting in the Dead Sea Rift, *Tectonophysics, 80*, 1-26, 1981.

Gibbs, A.D., Balanced cross-section constructions from seismic sections in areas of extensional tectonics, *J. Struct. Geol., 5*, 152-160, 1983.

Gilat, A., and A. Agnon, Geological map of the Ein Boqeq-Mezada area, scale 1:20,000, *Rep. MM/2/81*, Geol. Survey Isr., Jerusalem, 1981.

Ginzburg, A., and E. Kashai, Seismic measurements in the southern Dead Sea, *Tectonophysics, 80*, 67-80, 1981.

Harding, T.P., Divergent wrench fault and negative flower structure, Andaman Sea, Seismic expression of Structural styles, vol. 3, edited by A.W. Bally, *AAPG stud. geol., 15*, 4.2-1 to 4.2-8, 1983.

Harding, T.P., R.C. Vierbuchen, and N. Christie-Blick, Structural styles, plate-tectonic settings, and hydrocarbon traps of divergent (transtensional) wrench faults, in *Deformation and Basin Formation Along Strike-Slip Faults, Spec. Publ. 37*, edited by K.T. Biddle and N. Christie-Blick, pp. 51-77, Society of Economic Paleontologists and Minerologists, Tulsa, Okla., 1985.

Joffe, S., and Z. Garfunkel, Plate kinematics of the circum Red Sea- A reevaluation, *Tectonophysics, 141*, 5-23, 1987.

Johnson, N.M., C.B. Officer, N.D. Opdyke, G.D. Woodard, P.K. Zeitler, and E. H. Lindsay, Rates of Cenozoic tectonism in the Vallecito-Fish Creek basin, western Imperial Valley, California, *Geology, 11*, 664-667, 1983.

Kashai, E.L., The Dead Sea-Jordan rift system: Its tectonic framework, syntectonic sedimentation, and petroleum occurrence, Triassic and Jurassic Rifting in North America and North Africa, edited by W. Manspeizer, *Mem. Am. Assoc. Pet. Geol.* in press, 1989.

Kashai, E.L., and P.F. Crocker, Structural geometry and evolution of the Dead Sea-Jordan rift system as deduced from new subsurface data, *Tectonophysics, 141*, 33-60, 1987.

Mann, P., M.R. Hempton, D.C. Bradley, and K. Burke, Development of pull-apart basins, *J. Geol., 91*, 529-554, 1983.

Manspeizer, W., The Dead Sea Rift: impact of climate and tectonism on Pleistocene and Holocene sedimentation, in *Deformation and Basin Formation Along Strike-Slip Faults, Spec. Publ. 37*, edited by K.T. Biddle and N. Christie-Blick, pp. 143-158, Society of Economic Paleontologists and Minerologists, Tulsa, Okla., 1985.

Mitchum, R.M., Jr., P.R. Vail, and S. Thompson, Seismic stratigraphy and global changes of sea level, 2, The depositional sequence as a basic unit for stratigraphic analysis, Seismic Stratigraphy- Applications to Hydrocarbon Exploration, edited by C.E. Payton, *Mem. Am. Assoc. Pet. Geol. 26*, 53-62, 1977.

Muehlberger, W.R., Geology of northern Soledad basin, Los Angeles county, California, *Am. Assoc. Pet. Geol. Bull., 42*, 1812-1844, 1958.

Neev, D., and J. Emery, The Dead Sea, depositional processes and environments of evaporites, *Bull. Isr. Geol. Sur., 41*, 147 pp., 1967.

Neev, D., and J.K. Hall, Geophysical investigation in the Dead Sea, *Sediment. Geol., 23*, 209-238, 1979.

Picard, L., and U. Golani, Geological map of Israel, scale 1:250,000, northern sheet, Govt. Printer, Jerusalem, 1965.

Quennell, A.M., Tectonics of the Dead Sea Rift, in *20th International Geological Congress Mexico, Assoc. serv. Geol. Africa*, , 385-405, 1959.

Raz, E., Geological map of Ein Gedi, scale 1:50,000, Geol. Survey Isr., Jerusalem, 1986.

Reches, Z., Mechanical aspects of pull-apart basins and push-up swell with applications to the Dead Sea transform, *Tectonophysics, 141*, 75-88, 1987.

Rodgers, D.A., Analysis of pull-apart basin development produced by en echelon strike-slip faults, *Spec. Publ. Int. Assoc. Sedimentol., 4*, 27-41, 1980.

Rot, I., Geological map of Wadi el-Qilt, scale 1:50,000, Geol. Survey Isr., 1970.

Rotstein, Y., and E. Arieh, Tectonic implications of recent microearthquake data from Israel and adjacent areas, *Earth Planet. Sci. Lett., 78*, 237-244, 1986.

Sa'ar, H., Origin and sedimentation of sandstones in graben fill formations of the Dead Sea rift valley, *Rep. MM/3/86*, Geol. Survey Isr., Jerusalem, 1985.

Segall, P., and D.D. Pollard, Mechanics of discontinuous faults, *J. Geophys. Res., 85*, 4337-4350, 1980.

Steckler, M.S., and U.S. ten Brink, Lithospheric strength variations as a control on new plate boundaries: Examples from the northern Red Sea region, *Earth Planet. Sci. Lett., 79*, 120-132, 1986.

Vail, P.R., R.G. Todd, and J.B. Sangree, Seismic stratigraphy and global changes of sea level, 5, Chronostratigraphic significance of seismic reflections, Seismic Stratigraphy-Applications to Hydrocarbon Exploration, edited by C.E. Payton, *Mem. Am. Assoc. Pet. Geol., 26*, 99-116, 1977.

Wilcox, R.E., T.P. Harding and D.R. Seely, Basin wrench tectonics, *Am. Assoc. Pet. Geol. Bull., 57*, 74-96, 1973.

Yeats, R.S., Large-scale Quaternary detachments in Ventura Basin, southern California, *J. Geophys. Res., 88*, 569-583, 1983.

Zak, I., The geology of Mt. Sedom, Ph. D. thesis (in Hebrew, English abstract), 208 pp., Hebrew Univ., Jerusalem, 1967.

Zak, I., and R. Freund, Asymmetry and basin migration in the Dead Sea Rift, *Tectonophysics, 80*, 27-38, 1981.

Z. Ben-Avraham, Department of Geophysics and Planetary Sciences, Tel Aviv University, Ramat Aviv, 69978, Israel.

U.S. ten Brink, Department of Geophysics, Stanford University, Stanford, CA 94305.

(Received February 22, 1988
revised October 27, 1988
accepted November 4, 1988.)